DOI: 10.21122/2220-9506-2025-16-1-47-54

Detection of Hidden Defects Induced by Thermomechanical Processing of Aluminum Substrates for Sensor Devices Using a Scanning Kelvin Probe

A.L. Zharin[1], I.V. Gasenkova[2], A.K. Tyavlovsky[1], N.I. Mukhurov[2], S.I. Spitski[2]

[1]Belarusian National Technical University,
Nezavisimosty Ave., 65, Minsk 220013, Belarus
[2]SSPA "Optics, Optoelectronics, and Laser Technology",
Nezavisimosty Ave., 68-1, Minsk 220012, Belarus

Received 04.02.2025
Accepted for publication 11.03.2025

Abstract

The object of the study was aluminum substrates for creating sensor devices based on anodic aluminum oxide, which underwent mechanical processing in the form of grinding and straightening. The subject of the study was the detection of residual mechanical stresses and other surface defects to assess the quality of this processing using the scanning Kelvin probe technique. The technique applied allows for the effective detection of residual plastic deformations of aluminum substrates resulting from their mechanical processing with a resolution sufficient to detect mechanical stresses associated with individual roughnesses.

Keywords: aluminium substrates, thermomechanical treatment, scanning Kelvin probe, defect, roughness

Адрес для переписки:
Тявловский А.К.
Белорусский национальный технический университет,
пр-т Независимости, 65, г. Минск 220013, Беларусь
e-mail: andrey_psf@tut.by

Address for correspondence:
Tyavlovsky A.K.
Belarusian National Technical University,
Nezavisimosty Ave., 65, Minsk 220013, Belarus
e-mail: andrey_psf@tut.by

Для цитирования:
Zharin AL, Gasenkova IV, Tyavlovsky AK, Mukhurov NI, Spitski SI. Detection of Hidden Defects Induced by Thermomechanical Processing of Aluminum Substrates for Sensor Devices Using a Scanning Kelvin Probe.
Приборы и методы измерений.
2025. Т. 16. № 1. С. 47–54.
DOI: 10.21122/2220-9506-2025-16-1-47-54

For citation:
Zharin AL, Gasenkova IV, Tyavlovsky AK, Mukhurov NI, Spitski SI. Detection of Hidden Defects Induced by Thermomechanical Processing of Aluminum Substrates for Sensor Devices Using a Scanning Kelvin Probe.
Devices and Methods of Measurements.
2025;16(1):47–54.
DOI: 10.21122/2220-9506-2025-16-1-47-54

DOI: 10.21122/2220-9506-2025-16-1-47-54

Выявление скрытых дефектов алюминиевых подложек для сенсорных устройств после термомеханической обработки с помощью сканирующего зонда Кельвина

А.Л. Жарин[1], И.В. Гасенкова[2], А.К. Тявловский[1], Н.И. Мухуров[2], С.И. Спицкий[2]

[1]Белорусский национальный технический университет,
пр-т Независимости, 65, г. Минск 220013, Беларусь

[2]ГНПО «Оптика, оптоэлектроника и лазерная техника»,
пр-т Независимости, 68-1, г. Минск 220012, Беларусь

Поступила 04.02.2025
Принята к печати 11.03.2025

Объектом исследования являлись алюминиевые подложки для создания сенсорных устройств на основе анодного оксида алюминия, прошедшие механическую обработку в виде утонения, рихтовки и химической очистки поверхности. Предмет исследования – выявление остаточных механических напряжений, внутренних и поверхностных дефектов для оценки качества данной обработки методом сканирующего зонда Кельвина. Показано, что данный метод позволяет эффективно выявлять остаточные пластические деформации алюминиевых подложек, являющиеся следствием их термомеханической обработки, с разрешением, достаточным для выявления механических напряжений, связанных с отдельными шероховатостями.

Ключевые слова: алюминиевые подложки, термомеханическая обработка, сканирующий зонд Кельвина, дефект, шероховатость

Адрес для переписки:
Тявловский А.К.
Белорусский национальный технический университет,
пр-т Независимости, 65, г. Минск 220013, Беларусь
e-mail: andrey_psf@tut.by

Address for correspondence:
Tyavlovsky A.K.
Belarusian National Technical University,
Nezavisimosty Ave., 65, Minsk 220013, Belarus
e-mail: andrey_psf@tut.by

Для цитирования:
Zharin AL, Gasenkova IV, Tyavlovsky AK, Mukhurov NI, Spitski SI. Detection of Hidden Defects Induced by Thermomechanical Processing of Aluminum Substrates for Sensor Devices Using a Scanning Kelvin Probe.
Приборы и методы измерений.
2025. Т. 16. № 1. С. 47–54.
DOI: 10.21122/2220-9506-2025-16-1-47-54

For citation:
Zharin AL, Gasenkova IV, Tyavlovsky AK, Mukhurov NI, Spitski SI. Detection of Hidden Defects Induced by Thermomechanical Processing of Aluminum Substrates for Sensor Devices Using a Scanning Kelvin Probe.
Devices and Methods of Measurements.
2025;16(1):47–54.
DOI: 10.21122/2220-9506-2025-16-1-47-54

Introduction

When creating sensor devices based on nanoporous anodic aluminum oxide (AAO) and other functional systems, including that using the high-aspect nanostructured materials, the quality of not only the surface, but also the entire volume of the plate used as a substrate to form the anodic oxide plays a major role [1–5]. During the anodic oxidation process, aluminum parts undergo several successive processing stages: cleaning, thermomechanical treatment, etching, anodizing, and high-temperature annealing [6]. At the same time, the final surface treatment of the original aluminum plates, including electrochemical polishing, does not exclude the presence of undetected hidden defects in the form of residual plastic deformations, which, due to their unevenness, create mechanical stresses not only in the near-surface areas of the substrate. Such stresses are local and their detection requires mapping of the entire substrate surface, which should be carried out using a non-destructive, contactless method due to the high requirements for surface cleanliness in order to form anodic aluminum oxide with a porous structure which is identical in geometric parameters over the entire area.

This is especially important when creating photonic devices such as the Fabry–Perot interferometer, achromatic phase plates, and IR- and UV-to-visible converters [7–9].

One of the effective contactless techniques is the scanning Kelvin probe method, based on the registration of the contact potential difference (CPD) between the surface area of the sample and the sensitive element of the electrometric probe, which acts as two plates of a dynamic capacitor [10]. The method is characterized by an exceptionally high surface sensitivity, while the output measurement signal of a Kelvin probe is multiparametric [11] and reflects the parameters of both the chemical (composition heterogeneity, oxidation, presence of adsorbed substances and contaminants) and mechanical (presence of various crystal lattice defects, crystallographic orientation, presence of mechanical stresses and their sign, etc.) state of the surface. Because of that, additional information about the object of measurement is required to interpret the visualized image of CPD spatial distribution [12]. The aim of this study was to analyze the applicability of Kelvin probe technique for determining and distinguishing various types of defects induced by thermomechanical treatment of aluminum substrates used for precise applications like growing AAO structures and to advance methods of highly sensitive non-destructive testing of aluminum substrate surface.

Methods and equipment

The object of study in this work was aluminum substrates used for the manufacture of sensor devices based on anodic aluminum oxide.

The subject of the study was the identification of residual mechanical stresses and other surface defects to assess the quality of processing of relatively thick original aluminum plates. The high chemical homogeneity of the aluminum plates material (99,99 % Al) made it possible to interpret the results of scanning primarily as indicators of mechanical state of the surface.

The material was represented by aluminum plates of 0.6 mm thickness. To obtain a high-quality anodic aluminum oxide the roughness of aluminum plate surface should be at least class 10. To meet this requirement the aluminum strip was thinned using a rolling mill (Figure 1*a*). The rolling mill rolls have a surface finish class of at least 13, which assures the high quality of the aluminum foil surface after rolling (Figure 1*b*). A special attention was paid to the cylindricity deviation of a working surface of rolls and to the perfect matching of rolls' dimensions in pair. These parameters, along with the small runout of the rolls relative to the mounting necks, determine the minimum permissible thicknesses of the foils obtained from aluminum bars after rolling. The rolling process was accompanied by the use of a lubricant based on mineral oil ("spindle oil") and kerosene in a 1:1 proportion. During the operation of the rolling mill, the following parameters were ensured: roll runout relative to the mounting necks – no more than 5 μm, cylindricity deviation of the rolls' working surface – no more than 3 μm, discrepancy of the rolls' dimensions in a pair – no more than 5 μm, surface cleanliness of the rolls – no worse than class 13...14.

After rolling to the required thickness (≈ 100 μm) the aluminum band was cleaned from rolling lubricant traces using solvents (petrol, acetone) and finally by an isopropyl alcohol in an ultrasonic bath. The band prepared in this way was then cut into pieces measured 10×10 cm. Since after rolling and cutting the band into pieces the latter are not flat, then to impart their flatness the pieces were subjected to

straightening in a device consisting of straightening plates with working surfaces facing each other polished to 13th grade of cleanliness, heaters, and a device for clamping the plates (Figure 2). The device for thermal straightening and flattening of aluminum substrate samples provided the following parameters: heating temperature – 130–170 ºC, compressive force – $(10–20)\cdot10^6$ N/m^2.

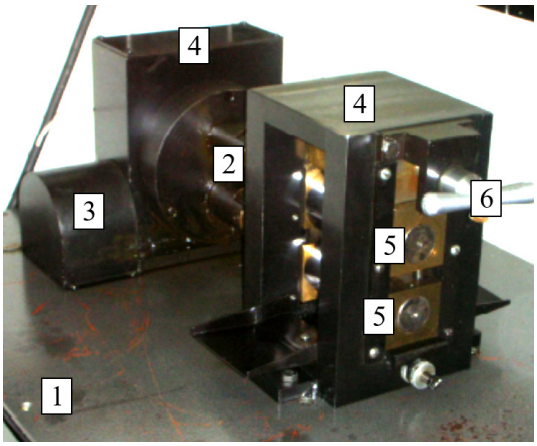

a

b

Figure 1 – General view of a rolling mill (*a*), and a view of rolls with high surface quality and low cylindricity deviation (*b*): 1 – rigid base with electric motor inside; 2 – rolls; 3 – roll rotation system; 4 – roll holder mounting housings; 5 – roll neck mounting devices; 6 – adjustment of gap between rolls

An important feature of straightening plates is that their coefficient of thermal expansion is approximately 2.5 times less than that of aluminum. The aluminum sample was placed between straightening plates, preheated to 150–250 °C, and the plates were compressed together. Due to the different coefficients of thermal expansion, during subsequent cooling in a clamped state the aluminum sample is subjected to plastic deformation uniformly in all directions, and the sample acquires a flat shape.

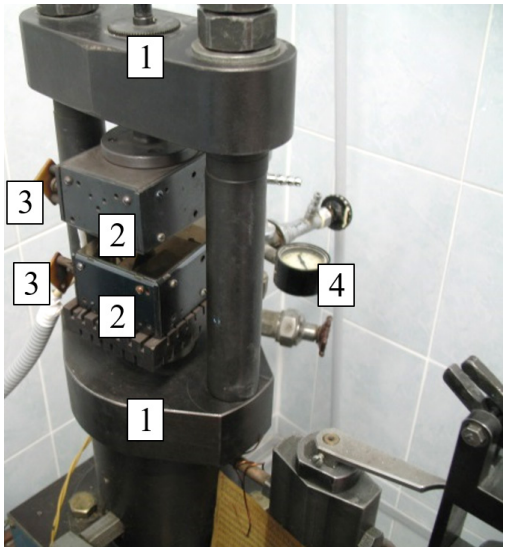

Figure 2 – Photo of the device for straightening and flattening of aluminum substrate samples: 1 – straightening plate holder; 2 – straightening plates; 3 – heaters; 4 – pressure control gauge

The methodology for studying the surface of aluminum substrates used for the formation of anodic aluminum oxide is based on the method of measuring the CPD with a dynamic capacitor (the Kelvin-Zisman technique). The technique is based on the phenomenon of the occurrence of electrostatic potentials difference between a conducting probe and a plate which surfaces have different values of the electron work function (EWF) φ_S and φ_P while ensuring conditions for the unimpeded exchange of charge carriers between them [10]. In accordance with the condition of thermodynamic equilibrium, in such case the Fermi levels will be equalized which leads to the emergence of an electrical potential difference. Kelvin–Zisman technique assumes using an active feedback in a form of compensating voltage source U_{CPD} connected in series with a dynamic capacitor formed by sample's surface and probe's tip which brings the current between surface and probe to zero. The equilibrium condition is:

$$eU_{CPD} + \varphi_S - \varphi_P = 0, \quad (1)$$

therefore:

$$U_{CPD} = \frac{\varphi_P - \varphi_S}{e}, \quad (2)$$

where e is elementary charge.

The U_{CPD} value describes the electrical potential difference between the surface of the sample under study and the probe's tip. It is important that in Kelvin–Zisman method the probe's output signal is determined by the mean EWF value of the sample surface φ_S in the area under study, and not by its minimum value as when using emission methods [13]. Since typical defect sizes for nanostructured surfaces are much smaller than the linear dimensions of the probe, such hardware averaging of the signal provides an integral assessment of the defects density in the area of study whereas emission methods provide a less diagnostically significant extreme estimate. Therefore scanning EWF measurements based on CPD registration with a Kelvin probe could be used to reveal surface defects of sensor components made of nanostructured materials and access the concentration (surface density) of these defects. In last decades, several researchers attempted to link the EWF to a certain physical properties of a material like Young's modulus [14] and yield strength [15], Young's modulus and hardness [16] of metals and alloys, and also a surface corrosion potential [17], with a mixed success. In particular, in the research work [14] there were proposed a theory-based mathematical model that numerically links the EWF φ with the Young's modulus E by a form of power-law dependence $E \sim \alpha\varphi^6$ where α is the Madelung constant. For real samples, however, all the mentioned and other factors (hardness and Young's modulus difference, surface contaminations, chemical composition variations, corrosion etc.) exist simultaneously and in unknown proportion which does not allow one to directly link the numerical walues of EWF or CPD with the values of specific physical parameters of the surface.

One should take into account that the value of φ_P in (1) is unknown since it cannot be determined by an independent method and can change under the influence of environmental factors, mainly due to the adsorption of various substances on the probe's tip. As these changes are relatively slow, the φ_P value may be considered constant all over the time of scanning when measuring surface CPD with a Kelvin probe. In this case, the difference in the measured values of the electrostatic potentials in two adjacent points will be:

$$\Delta U_{CPD} = U_{CPD1} - U_{CPD2} = \frac{\varphi_P - \varphi_{S1}}{e} - \frac{\varphi_P - \varphi_{S2}}{e} = \frac{\varphi_{S2} - \varphi_{S1}}{e}. \quad (3)$$

The equivalence of CPD and EWF differencies indicates that visualized CPD distribution map provided by scanning Kelvin probe technique objectively reflects the inhomogeneities of EWF distribution and can be used to compare the degree of defectiveness (or surface defect density) of different areas of the sample surface. If the vast part of the surface under study is considered defect-free then any part of a surface where CPD deviates from the mean CPD value for a given sample can be considered as a host for defects of some origin.

It should be noted that output signal of a scanning Kelvin probe is virtually independent of a probe-to-sample gap, which only affects the spatial resolution of the probe and the signal-to-noise ratio [18], so particular features of CPD distribution map shouldn't be treated as geometric deviations of the surface shape. The research was performed using a laboratory model of a microprocessor based measuring transducer of electrostatic potentials with high spatial resolution for monitoring the microstructure of the mesh web, developed within the framework of Event 2.3 of the Union State program "Monitoring-SG" (Figure 3) and used in the BNTU Semiconductor Technology Research Laboratory, and a proprietary software [19].

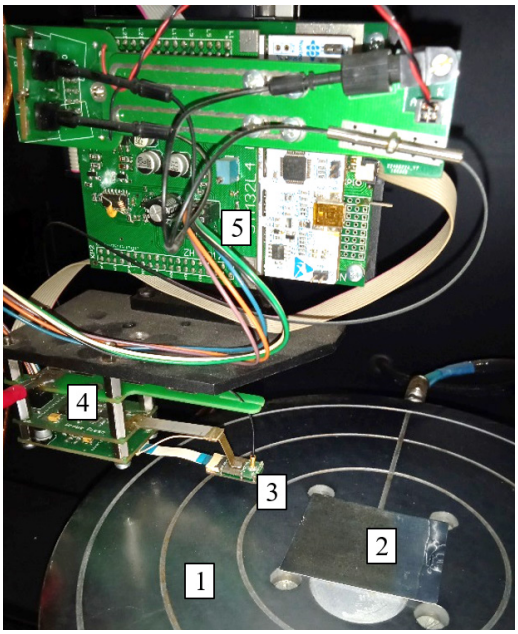

Figure 3 – Microprocessor based scanning measuring transducer of electrostatic potentials (Kelvin probe) that was used in the research: 1 – sample holder attached to scanning system; 2 – sample; 3 – electrometric probe; 4 – Kelvin probe driver and signal preamplifier; 5 – microprocessor based measuring transducer

Results and discussion

The obtained spatial CPD distributions of the samples under study are given on Figures 4–6. The coordinates along the *X* and *Y* axes are given in millimeters; *Z* axis that reflects the CPD values on the three-dimensional representation of the CPD distribution is scaled in millivolts.

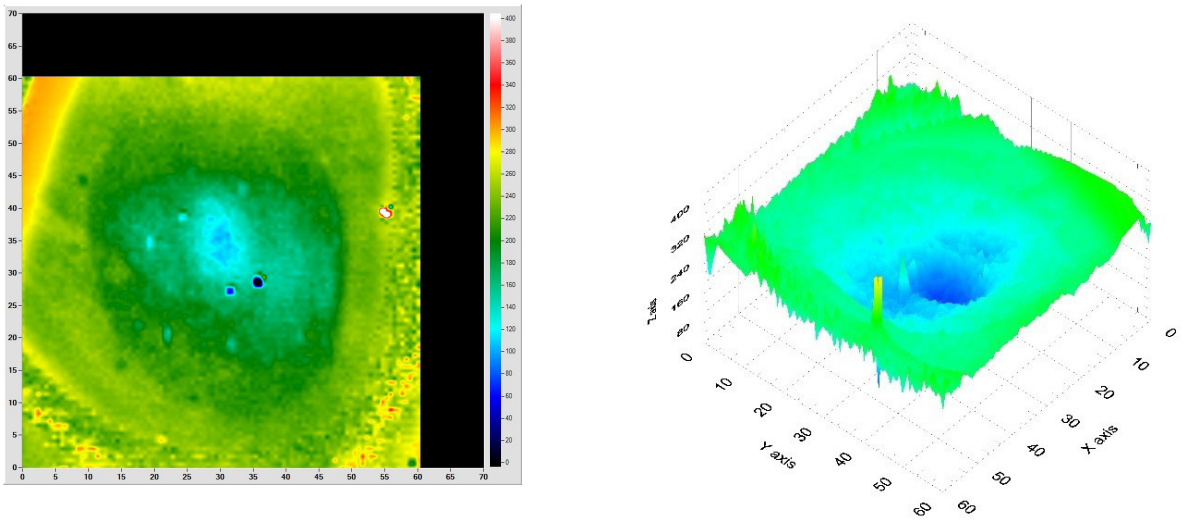

a *b*

Figure 4 – Spatial contact potential difference distribution of a sample with a nominal surface roughness of 200 nm: *a* – visualized map of contact potential difference distribution; *b* – 3D graph of contact potential difference distribution

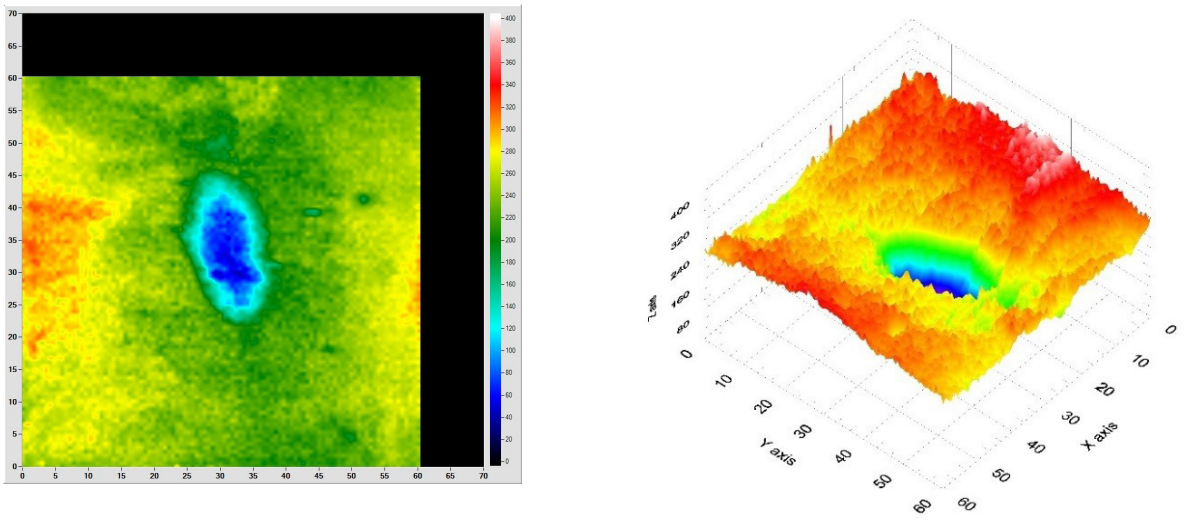

a *b*

Figure 5 – Spatial contact potential difference distribution of a sample with a nominal surface roughness of 300 nm: *a* – visualized map of contact potential difference distribution; *b* – 3D graph of contact potential difference distribution

In general, the results of the studies showed that CPD values do not depend on the magnitude of the surface roughness and amount to an average of 240 mV in the non-deformed areas of all the studied samples. At the same time, in the areas of plastic deformations after straightening all samples demonstrated a significant decrease in the recorded CPD values to 40–80 mV, which corresponds to an increase in the relative EWF values by 160–200 meV. Typical in this regard is the spatial CPD distribution map of an aluminum plate with a roughness of 200 nm shown in Figure 4*a*.

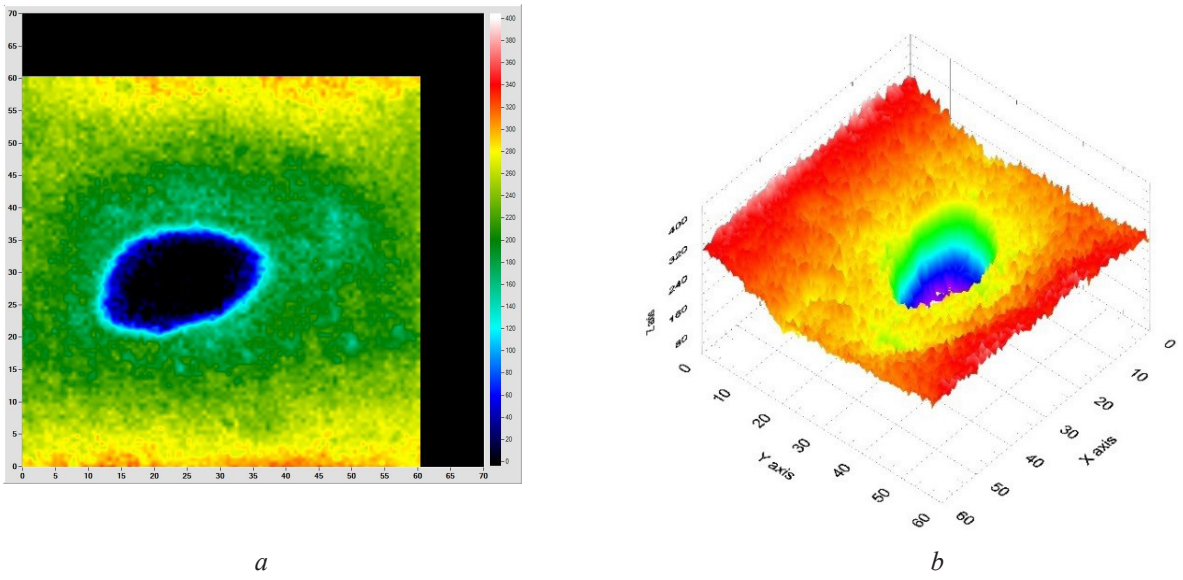

a *b*

Figure 6 – Spatial contact potential difference distribution of a sample with a nominal surface roughness of 400 nm: *a* – visualized map of contact potential difference distribution; *b* – 3D graph of contact potential difference distribution

The image demonstrates the "stepwise" change in CPD values corresponding to several successive stages of rolling. The better observation and analysis of these effects is provided by the three-dimensional representation of spatial CPD distribution shown in Figure 4*b*. The prominent irregularities (fluctuations) of CPD values characterized with a small amplitude and high spatial frequency can be attributed to the resolution of individual roughnesses by a high-resolution Kelvin probe, the peaks and valleys of which are also concentrators of mechanical stress. This effect is more clearly manifested for surfaces with a greater roughness height and step, which can be observed in the images of Figures 5 and 6. Therefore the visualized potential map to a certain extent reflects the geometric relief of the surface, in this case in the form of surface roughness.

In addition to relatively large areas of mechanical stress where EWF values an increased, there are several local points on the visualized the maps where EWF values differ sharply from that of the surrounding surface, both to the higher and to the lower side. Most obviously such points can be traced on a visualized map given on Figure 4*a*, in particular in the central part of the sample. The arbitrary (either positive or negative) sign of EWF shift, high locality and apparent lack of correlation between position of these points and sites of possible residual mechanical stresses after the rolling and straightening allows us to suggest that these local EWF irregularities represent point surface contamination that caused a local change in the surface EWF due to the interaction of the adsorbed contaminant with the aluminum surface, and not the mechanical defects.

It is significant that creation of a complete visualized CPD distribution map of the whole surface made it possible to identify various types of defects, including those that appear at the microscopic level (individual roughnesses, surface contamination). Additionally, the overlapping defects such as not completely coinciding areas of work hardening after several rolling stages, are clearly distinguishable and can be easely identified in the macroscopic image.

Conclusion

The results of the studies showed that the scanning Kelvin probe method allows for the effective detection of residual plastic deformations of aluminum substrates resulting from their thermomechanical processing. The achieved spatial resolution of the scanning Kelvin probe probe was sufficient for resolving individual roughnesses which acts as microconcentrators of mechanical stresses. The multiparametric nature of the scanning Kelvin probe signal in the conditions of simultaneous presence of various types of defects does not allow for determining an unambiguous link between the results of local contact potential difference measurements and specific quantitative characteristics of the surface. On the other hand, studies carried out on a macroscopic scale using high spatial resolution scanning allow us

to identify and qualitatively characterize (typify) defects of various natures (in the particalar case that where residual plastic deformations after several successive stages of rolling, individual roughness, and local surface contamination) and to determine their exact location.

References

1. Losic D, Voelcker NH. Nanoporous anodic aluminium oxide: Advances in surface engineering and emerging applications. Progress in Materials Science. 2013;58(5):636-704.
DOI: 10.1016/j.pmatsci.2013.01.002

2. Santos A, Kumeria T, Losic D. Nanoporous Anodic Aluminum Oxide for Chemical Sensing and Biosensors. TrAC Trends in Analytical Chemistry. 2013;44:25-38. **DOI:** 10.1016/j.trac.2012.11.007

3. Feng S, Ji W. Advanced Nanoporous Anodic Alumina-Based Optical Sensors for Biomedical Applications. Frontiers in Nanotechnology. 2021;3:678275-18.
DOI: 10.3389/fnano.2021

4. Liu S, Tian J, Zhang W. Fabrication and application of nanoporous anodic aluminum oxide: A review // Nanotechnology. 2021;32(22):222001-20.
DOI: 10.1088/1361-6528/abe25f

5. Ku C.-A. [et al.] Advances in the Fabrication of Nanoporous Anodic Aluminum Oxide and Its Applications to Sensors: A Review. Nanomaterials. 2023;13(21):(42): 2853-2895. **DOI:** 10.3390/nano13212853

6. Gasenkova IV, Mukhurov NI, Zhvavyi SP, Kolesnik EE. Optical characteristics of Cr_2O_3/Al_2O_3 composite structure. High Temperature Material Processes. 2021;25(3):1-10.

7. Gasenkova IV, Mukhurov NI, Andruhovich IM. Parameters of anodic aluminum oxide determined from Fabry-Perot oscillations in specular reflectance spectra. BSUIR Reports. 2024;22(6):14-20.
DOI: 10.35596/1729-7648-2024-22-6-14-20. (In Russ.)

8. Dlugunovich VA. [et al.]. Conversion of light polarization using nanoporous aluminum oxide films. Journal of Applied Spectroscopy. 2015;82(5):766-772. (In Russ.).

9. Yasin Mahsin Vahioh [et al.]. Threshold detectors of ionizing and ultraviolet radiation based on nanostructured substrates made of anodic aluminum oxide. Edited by N.I. Mukhurov. Minsk: Bestprint. 2016:178 p.

10. Melitz W. [et al.]. Kelvin probe force microscopy and its application. Surf. Sci. Rep. 2011;66:1-27.

11. Hui X. [et al.]. Multiparametric Kelvin Probe Force Microscopy for the Simultaneous Mapping of Surface Potential and Nanomechanical Properties. Langmuir. 2017;33(11):2725-2733.
DOI: 10.1021/acs.langmuir.6b04572

12. Findlay A. [et al.]. Non-Visual Defect Monitoring with Surface Voltage Mapping. ECS Journal of Solid State Science and Technology. 2015;5(4):3087-P3095.
DOI: 10.1149/2.0161604jss

13. Ibragimov HI, Korolkov VA. Electron work function in physical and chemical research. Moscow: Intermet Engineering, 2002;526 p. (In Russ.).

14. Hua G, Li D. Generic relation between the electron work function and Young's modulus of metals. Applied Physics Letters. 2011;99:041907-3.
DOI: 10.1063/1.3614475

15. Hua G, Li D. The correlation between the electron work function and yield strength of metals. Phys. Status Solidi B. 2012;249(8):1517-1520.
DOI: 10.1002/pssb.201248051

16. Lu H, Hua G, Li D. Dependence of the mechanical behavior of alloys on their electron work function – An alternative parameter for materials design. Applied Physics Letters. 2013;103(26):261902-4.
DOI: 10.1063/1.4852675

17. Liew Y. [et al.]. In Situ Time-Lapse SKPFM Investigation of Sensitized AA5083 Aluminum Alloy to Understand Localized Corrosion. J. Electrochem. Soc. 2020;167:141502–11.
DOI: 10.1149/1945-7111/abc30d

18. Zerweck U. [et al.]. Accuracy and resolution limits of Kelvin probe force microscopy. Phys. Rev. B. 2005;71:125424. **DOI:** 10.1103/PhysRevB.71.125424

19. Tyavlovsky KL. [et al.]. Surface electric potential measurement with a static probe. Devices and Metods of Measurement. 2023;14(2):135-144. (In Russ.).
DOI: 10.21122/2220-9506-2023-14-2-135-144